Direct Visualization of Single Ions in the Stern layer of Calcite.

Maria Ricci[†], *Peter Spijker*[†§], *Francesco Stellacci*[†], *Jean-Francois Molinari*[†] *and Kislon Voïtchovsky*[†*]

[†]Department of Materials Science and Engineering, École Polytechnique Fédérale de Lausanne (EPFL), 1015 Lausanne, Switzerland

[§]COMP Centre of Excellence, Aalto University, Department of Applied Physics, P.O. Box 11100, FI-00076, Helsinki, Finland

KEYWORDS: Calcite, Atomic Force Microscopy, Single ions, Stern layer, Molecular Dynamics Simulation.

TABLE OF CONTENT GRAPHIC

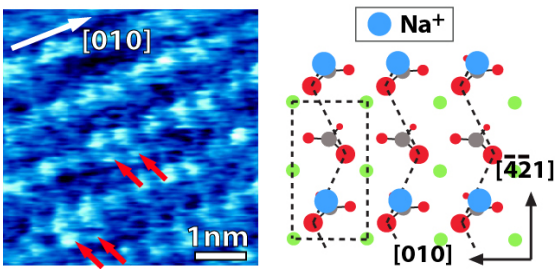

ABSTRACT

Calcite is among the most abundant minerals on earth and plays a central role in many environmental and geochemical processes. Here we used amplitude modulation atomic force microscopy (AFM) operated in a particular regime to visualize single ions close to the $(10\bar{1}4)$ surface of calcite in solution. The results were acquired at equilibrium, in aqueous solution containing different concentrations of NaCl, RbCl and $CaCl_2$. The AFM images provide a direct and atomic-level picture of the different cations adsorbed preferentially at certain locations of the calcite-water interface. Highly ordered water layers at the calcite surface prevent the hydrated ions from directly interacting with calcite due to the energy penalty incurred by the necessary restructuring of the ions' solvation shells. Controlled removal of the adsorbed ions from the interface by the AFM tip provides indications about the stability of the adsorption site. The AFM results show the familiar "row-pairing" of the carbonate oxygen atoms, with the adsorbed monovalent cations located adjacent to the most prominent oxygen atoms. The location of adsorbed cations near the surface appears better defined for monovalent ions than for Ca^{2+}, the latter being easily moved by the measuring AFM tip. This is consistent with the idea that Ca^{2+} ions remain further away from the surface of calcite due to their larger hydration shell. The precise distance between the different hydrated ions and the surface of calcite is quantified using MD-simulation. The preferential adsorption sites found by MD as well as the ion residence times close to the surface support the AFM findings, with Na^+ ions dwelling substantially longer and closer to the calcite surface than Ca^{2+}. The results also bring new insights into the problem of the Stern and electrostatic double layer at the surface of calcite, showing that some important parameters such as the thickness of the Stern layer can be highly ion-dependent.

1. INTRODUCTION

Calcite ($CaCO_3$) is among the most abundant minerals on earth, counting for more than 4% of the earth's crust.[1] This crystalline rock plays a central role in many environmental[1-3] and geochemical processes.[4] It is widely used in industry, with applications in fields as diverse as paper and cement production, nuclear waste storage, optics components, waste-water treatment[5] and oil extraction with calcareous rocks containing more that 40% of known oil reserves, often mixed with water and ions.[6] The vast majority of these processes strongly depend on reactions occurring at the interface between the surface of calcite and a surrounding aqueous environment. Water molecules,[7,8] ions,[3,9,10] biomolecules[11] or organic components[12] can all interact with calcite's surface, influence its morphology, crystalline growth and dissolution as well as its structural properties.[13-16] Numerous theoretical and experimental studies have explored these interfacial processes, generally focusing on the $(10\bar{1}4)$ cleavage plane of calcite, the most stable and abundant of calcite's facets[1]. The crystalline structure of bulk calcite and of the $(10\bar{1}4)$ cleavage plane is presented in figure 1A. Calcite possesses a trigonal-rombohedral (R $\bar{3}$2/m space group)[17] with both calcium and carbonate ions forming a rectangular lattice in the $(10\bar{1}4)$ plane. The carbonate groups are however tilted with respect to the plane,[1,7] with one oxygen atom protruding above the plane and the others lying below (Fig. 1A). Furthermore, every carbonate along the $[\bar{4}\bar{2}1]$ direction is rotated by 180° resulting in a characteristic zigzag pattern along this direction (highlighted in Fig. 1A-B), often reported in atomic force microscopy (AFM) studies.[18-22]

Most experimental investigations rely on surface- or interface-sensitive techniques such as low-energy electron diffraction,[23] X-ray reflectivity,[8,24] photoelectron spectroscopy,[7,23] and

AFM.[18-22] AFM's ability to probe samples locally with atomic-level resolution and in a liquid environment has established the technique as a tool of choice to study calcite growth and dissolution in different saline and pH environments.[13,14,20,22,25-29] *In-situ* real-time AFM experiments have explored the nucleation and kinetics of surface kinks and steps[30] as a function of the Ca^{2+} to CO_3^- concentration ratio, a factor often used to characterize oceanic and continental waters super-saturated with calcite.[31] The presence of different background electrolytes[32] as well as particular ions such as Li^+, Sr^{2+}, Mg^{2+} and Ba^{2+} have been shown to influence the progression of acute or obtuse steps, sometimes specifically.[9,14,26,33-36] Organic molecules can have similar effects on the surface of calcite,[37,38] with obvious consequences for bio-mineralization and oil extraction.

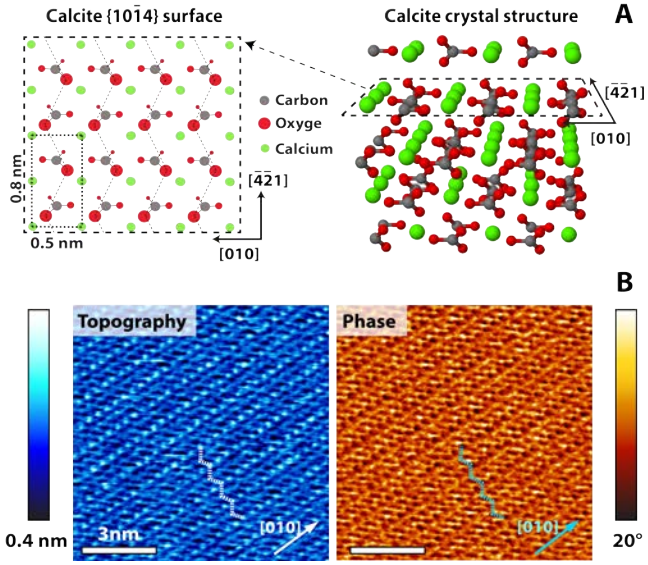

Figure 1. (A) Crystal structure of calcite. The atomic arrangement of the calcium and carbonate ions is shown for the bulk crystal (right) and the (10$\bar{1}$4) surface (left), together with the main crystallographic directions and a possible unit cell. The zigzag patterns of the protruding oxygen atoms of the (10$\bar{1}$4) surface are evidenced with thin dotted lines. (B) Typical amplitude-modulation AFM image of the (10$\bar{1}$4) surface equilibrated with ultrapure water. Both the

topography and phase image are shown. The previously reported "row-pairing"[18-20,22,39] is clearly visible in the topography with every other row of oxygen atoms along the $[\bar{4}\bar{2}1]$ direction appearing more prominent. The origin of this surface reconstruction, routinely reported in AFM studies, is still debated in the literature[19]. At the present time its real nature remains controversial and no reconstruction was shown in the crystal structure presented in (A). The zigzag structure is indicated by a dotted line in both images.

Most AFM studies, however, are primarily focused on the reactions and surface dynamics occurring out of equilibrium at calcite's atomic step-edges. Furthermore, investigations providing an atomic-level description of both the calcite surface and the interacting molecule or ion considered are scarce, especially in conditions near equilibrium. Although experimentally more challenging, this type of investigation can provide valuable insights into slowly evolving systems such as oceanic floors and oil reservoirs where water, ions and organic molecules are in contact mainly with calcite's $(10\bar{1}4)$ surface.[6] Away from steps, the crystallographic alternate arrangement of calcium and carbonate at the $(10\bar{1}4)$ surface of calcite (Fig.1A) induces strong local variations in surface charge. This charge distribution is particularly suitable for adsorbed water molecules that can orient with their oxygen facing the calcium and their hydrogen atoms oriented toward the carbonates.[3,7] As a result, the surface is unusually hydrophilic, with several nanometers of water even in dry environments.[29] Most small charged molecules or ions have to pay a substantial energetic penalty to reach calcite's surface. This penalty has an entropic origin and represents the cost of stripping the molecule from its hydration shell as it transverses the surface-bound water layers.[40] Experimentally, this effect makes the observation of single ions interacting with the surface of calcite in solution particularly challenging and most available results rely on diffraction techniques.[1]

Here we used amplitude modulation AFM (AM-AFM) operated in a particular regime to visualize single ions close to the $(10\bar{1}4)$ surface of calcite in solution. In this regime, the AFM tip is oscillated within the interface formed by calcite with the liquid, without significantly interacting with (tapping on) the calcite surface. The aim of the approach is to probe the whole interface by ensuring that most of the energy dissipated by the vibrating tip occurs within the interfacial liquid. This is achieved using oscillation amplitudes comparable to the size of the interface (0.5nm - 1nm) with a relatively soft cantilever (k = 0.1-0.8 N/m) and with a ratio between imaging and free amplitude typically larger than 0.8.[41] The results were acquired at equilibrium, in aqueous solution containing different concentrations of NaCl, RbCl and $CaCl_2$. The AFM images provide a direct picture of the different ions 'adsorbed' preferentially at certain locations of the calcite-water interface. The ions do not directly bind to the calcite surface due to water molecules remaining in-between at all times. Controlled removal of these hydrated ions from the interface by the scanning AFM tip provides indications about the stability of the adsorption site. We study Na^+ and Ca^{2+} for their abundance in oceans and rivers, and Rb^+ is used as a control. Our AFM results show the familiar "row-pairing" of the carbonate oxygen atoms,[18,20,22,39] with the adsorbed monovalent cations located adjacent to the more protruding oxygen atoms. The location of adsorbed cations near the surface appears better defined for monovalent ions than for Ca^{2+}, the latter being easily moved by the measuring AFM tip. This is consistent with the idea that divalent ions remain further away from the surface of calcite due to their larger hydration shell. The precise distance between the different hydrated ions and the surface of calcite is quantified using MD-simulation. The preferential adsorption sites found by MD as well as the ion residence times close to the surface support the AFM findings, with Na^+ ions dwelling substantially longer and closer to the calcite surface than Ca^{2+}. Additionally the

results bring new insight into the problem of the Stern and electrostatic double layer at the surface of calcite, revealing how the thickness of Stern layer and effectively the sphere of complexation of the ions at the surface can strongly depend on the ionic species involved.

2. MATERIALS AND METHODS

2.1 Molecular Dynamics Simulations.

From previous experiments and simulations, the coordinates of the atoms were obtained within a single unit cell in the calcite crystal with the $(10\bar{1}4)$ plane exposed.[42,43] A calcite crystal of 14x14x14 unit cells was constructed with a final dimension of 105x64x40 $Å^3$. As the molecules that make up the calcite-water system (carbonate, calcium, water and ions) are of a biological nature, the empirical force field CHARMM was used in all computations,[44-46] which were carried out using the molecular dynamics code NAMD.[47]

After the creation of the initial calcite crystal, several short minimization and relaxation simulations (in the NPT-ensemble) were performed to stabilize the system. Once a stable calcite crystal was obtained, the system was solvated on the side of the $(10\bar{1}4)$ plane, keeping the periodic boundaries in mind. Approximately 68,000 water molecules were introduced to the system, enlarging the z-dimension to 108 Å. Besides water molecules, 100 ion-pairs (either NaCl or $CaCl_2$) were also added to the water phase of the system, giving a molarity of ~250 mM. For each ion-pair 10 different set-ups were constructed to improve statistical accuracy, each with the 100 pairs placed at different random locations and different initial velocities. Besides short minimization and equilibration runs, the production run covered 5 ns in real time at ambient

conditions (310 K and 1 bar). The simulations were run in parallel on a typical Linux commodity cluster.

Analysis of the simulations were performed either visually using VMD[48] or numerically using the Python library MDAnalysis[49] and Matlab.

2.2 Sample preparation for AFM.

Optically clear, Island Spar calcite samples were used for this study. The samples were cleaved with a razor blade and incubated in ~15 ml of the relevant aqueous solution for more than 24 h before being used so as to allow the system to equilibrate. All the solutions were made with ultrapure water (18.2 ΩM, <4 ppb organics, Merck-Milipore, Billerica, MA, USA) and each solution contains only one type of salt, NaCl, $CaCl_2$ or RbCl. In order to ensure that equilibrium was effectively reached, we measured the pH of the solution after equilibration and compared with corresponding theoretical calculations (using the free software PREEQC). We generally found a good correspondence between the measured and calculated values although deviations can be found for certain values. We attribute these errors to the small experimental volumes, which can make pH measurements challenging. For calcite equilibrated in ultrapure water, the measured and calculated pH values were of 8.4±0.1 and 8.24 respectively. The pH obtained for calcite equilibrated in solutions containing added salt are summarized in table 1 below.

	NaCl		$CaCl_2$		RbCl
Conc.	Meas.	Calc.	Meas.	Calc.	Meas.
1mM	8.0	8.25	8.0	8.05	8.8
5mM	8.0	8.26	-	7.80	8.8
10mM	7.9	8.27	7.6	7.69	8.7

50mM	7.9	8.29	-	-	8.5
100mM	8.3	8.31	-	-	9.1

Table 1: Measured and calculated pH values for calcite equilibrated in the different salt solutions used in this study. The experimental error for each measurement is typically ±0.1. No calculated pH values are available for calcite in RbCl.

The samples were then mounted onto a stainless steel support and loaded into the AFM. Attention was paid to always keep the surface of calcite in contact with liquid from the equilibrated solution. More solution (~150 µl) was added prior to imaging.

When calcite is equilibrated with ultrapure water, the ionic strength of the resulting solution is typically 1.5×10^{-3} in normal atmospheric conditions, mainly due to the presence of dissolved calcium and carbonate ions in the solution. Although the AFM images obtained in these conditions (Fig. 1B) appear comparable to results achieved in ultra high vacuum,[19] the dissolved ions may still play a role in the imaging and interact with the negatively charged AFM tip.[22] In order to avoid any ambiguity in the interpretation of the AFM results derived in the presence of added salt, we systematically varied the ionic concentration of the salt so as to identify consistent trends. This strategy also allows a more robust comparison of the results in the different salts.

2.3 AFM measurements.

All the measurements were carried out in liquid with a commercial Multimode Nanoscope IIIA (Digital Instruments, now Brucker, Santa Barbara, CA, USA) equipped with an external lock-in amplifier. We used standard silicon nitride cantilevers (RC800-PSA, Olympus, Japan) with a nominal stiffness k_c=0.76 N/m. The cantilevers were mounted in a fluid cell and fully immersed

into the liquid for the experiment. The system was allowed to thermalize at room temperature (24±2°C) for 30 to 60 minutes before acquiring any data so as to minimize drift. The liquid cell was equipped with an O-ring to limit evaporation of the liquid and imaging conditions were routinely kept stable for several hours without need for liquid to be added to the cell. The AFM was operated in amplitude-modulation mode ('tapping' in the AFM commercial software) with free amplitudes A_0 typically smaller than 1.5 nm and imaging amplitudes A so as to keep the setpoint ratio A/A_0 as high as possible (typically $A/A_0 \geq 0.8$). Operated in these conditions, the AFM tip mostly probes the interfacial liquid interacting with the surface of the solid, without directly and significantly interacting with the solid itself.[41,50,51] The images therefore represent the solvation structure formed by the water and the adsorbed ions at the surface of the calcite. The phase images provide an indication about the local solvation free energy with darker contrasts revealing local maxima.[41]

Image analysis was performed using SPIP (Image Metrology, Denmark). The images were flattened and lightly low-pass filtered. Amplitude and phase versus distance curves were acquired in each experiment and subsequently analyzed using routines programmed in Igor Pro (Wavemetrics, Lake Oswego, OR, USA).

3. RESULTS AND DISCUSSION

3.1 Molecular Dynamics Simulation of ions in solution at the surface of calcite.

One of the major strengths of MD simulations is the ability to provide insight at atomic length and time scales simultaneously, making it possible to follow individual atoms and look at local structures, such as the calcite-water interface. MD simulations of the calcite-water systems

showed a strong ordering of water near the calcite surface (see Fig. 2(A)), as expected from the experiments and literature.[7] The computed density profiles (see Fig. 2(B)) perpendicular to the surface correspond well with comparable X-ray scattering measurements[8] or other numerical simulations.[42,52]

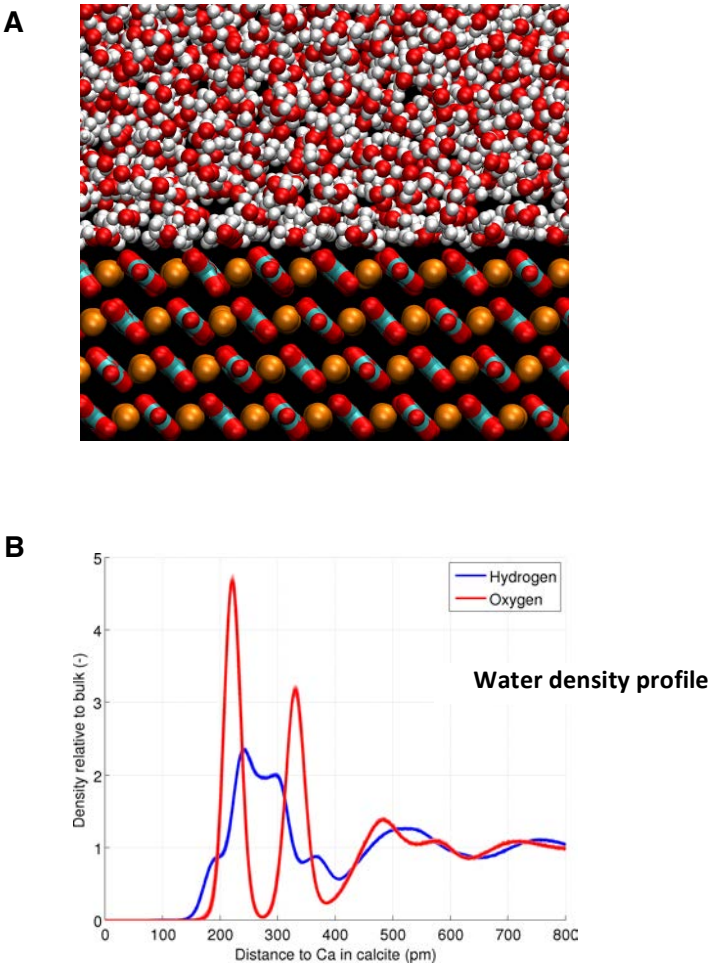

Figure 2. (A) Snapshot of the simulated calcite-water interface. The calcium (orange) and carbonates (red/blue) of the calcite crystal are visible. The oxygen and the hydrogen of the water molecules are depicted in red and white respectively. Ions in solution have been omitted for clarity. (B) Water density perpendicular to the calcite surface, with the density for oxygen atoms

in red and for hydrogen atoms in blue. The density is normalized with respect to the density in the bulk water phase and the surface calcium atoms are used as a reference for the distance measurement.

The density of the oxygen atoms of water molecules in the first and second layer parallel to the calcite surface (see Fig. 3(A)) shows the typical structure observed in AFM experiments (e.g. Fig.1), including the zigzag structure of the calcite surface. Although a density profile is not the same as the topography and phase images obtained from AFM measurements, their resemblance is striking and gives at least qualitative insight. A more careful examination of Fig. 3(A) reveals two vertical rows (around 1 nm and 7 nm) where the zigzag structure is broken.

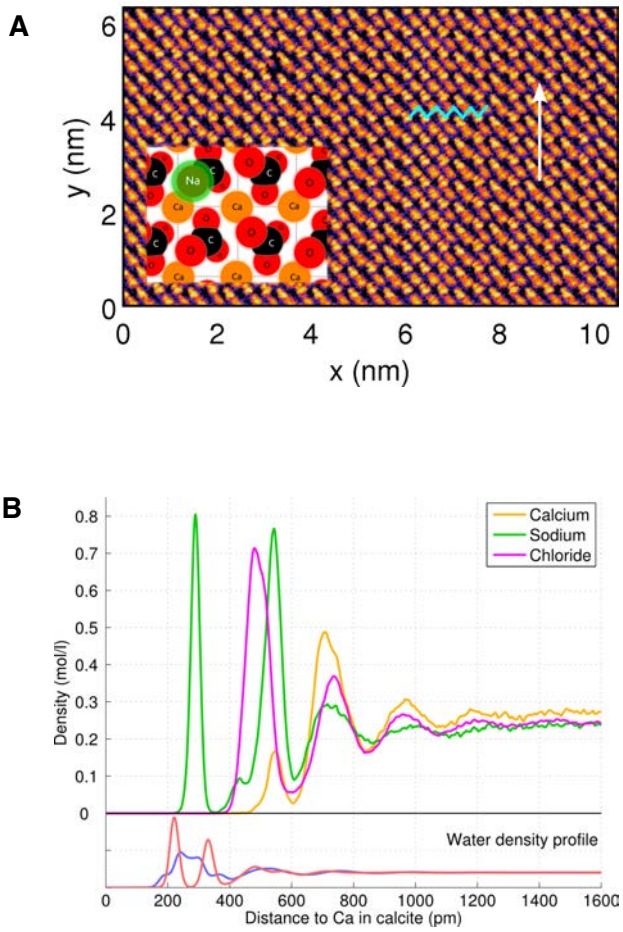

Figure 3. (A) Density distribution for oxygen atoms (H_2O) in the first and second structured layer parallel to the calcite surface. The zigzag structure ascribable to the calcite surface is indicated as well the [010] direction (white arrow). The inset shows schematically sodium ions closest to the surface being typically located above the nearby oxygen of the carbonate group. (B) Density profiles (mol/l) for three different ions (Na^+, Ca^{2+} and Cl^-) perpendicular to the calcite surface. The density of the water atoms is given at the bottom for comparison (see also Fig. 2(B)).

A thorough analysis of the trajectory of the simulations revealed that during the minimization and relaxation of the crystal structure, one carbonate molecule in each of these two rows spontaneously swapped, subsequently forcing the entire row to swap as well. The applied barostat imposed during the remainder of the simulations prevented this from reoccurring. Although not of direct significance in the present results, the actual swapping process is nevertheless interesting and deserves some more detailed analysis in the future, especially in light of the current debate about the reconstruction of calcite's surface[18]. In the same figure the inset shows schematically the location of the sodium ions when closest to the surface: above the oxygen atoms of carbonate protruding above the calcium-carbon plane.

The concentration of ions used in the MD simulations is high (~250 mM) when compared to the experiments. This strategy was applied in order to get sufficient statistics in the short time scale of the simulations; a substantial number of ions are needed to be able to make contact with the calcite-water interface. Combining the results from all 10 independent runs for each ion-pair allowed for the computation of a clean density distribution perpendicular to the surface (see Fig. 3(B)). These density distributions correspond well with previous numerical simulations of similar systems.[53,54] The density distributions show that neither ion manages to penetrate the

final water layer so as to reach the calcite surface. Sodium gets closest but remains on top of the first water layer. Calcium ions mostly remain outside calcite's structured water. To clarify these results a 2D-density distribution of water perpendicular to the surface is shown in figure 4, where the locations of several arbitrary but representative ions found close to the interface are indicated as well.

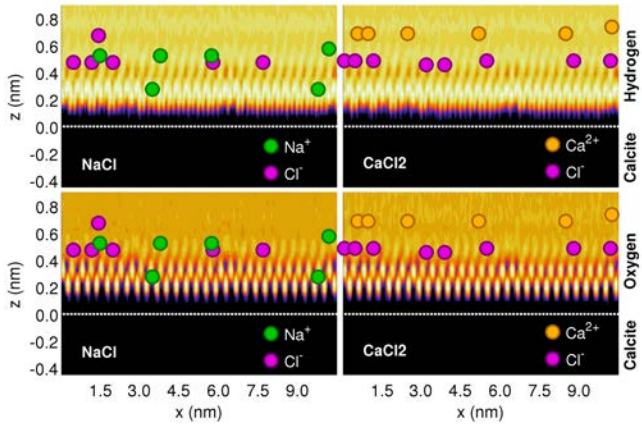

Figure 4. Two-dimensional density distribution of the hydrogen (top) and oxygen (bottom) atoms of water derived from Molecular Dynamic simulations. The view is taken perpendicular to the calcite surface and the x-direction of the calcite crystal (see Fig. 3A) is taken along the bottom axis. The brighter colors (yellow) represent higher densities for a given location. A clear multilayered structure is visible (up to three layers are easily visible). Sites corresponding to high concentrations of ions (Na^+, Ca^{2+}, Cl^-) are indicated by the colored circles (orange Ca^{2+}, green Na^+, and purple Cl^-). Sodium clearly gets closer to the surface than any of the other ions. The dotted white line indicates the plane containing the calcium atoms of calcite's surface. This plane is used as the origin of distance measurements on the z-axis.

3.2 AFM of calcite in Sodium Chloride.

The $(10\bar{1}4)$ surface of calcite imaged in the presence of added NaCl is shown in figure 5. At 1 mM NaCl (see Fig.5E) the calcite surface appears very similar when imaged in equilibrated pure water (Fig.1B), with the "row-pairing" showing alternated rows of 'prominent' and 'sunken' protrusions attributed to the oxygen atoms along the $[\bar{4}\bar{2}1]$ direction. For the sake of clarity these terms ('prominent' and 'sunken') will be used throughout this paper for designating the respective rows of protruding oxygens when the "row pairing" is visible. The attribution of the main visible features to oxygen atoms is consistent with the surface structure of calcite and compatible with the MD results as well as with published AFM literature.[18,20,22,39]

At 5 mM NaCl, the apparent surface of calcite remains unchanged (not shown). At 10 mM NaCl, the prominent oxygen rows sometimes appear broader locally (Fig.5A, red arrows), induced by additional protrusions locally appearing on the surface. These protrusions are however weakly bound to the surface and can easily be removed by increasing the force exerted by the AFM tip on the surface (effectively lowering the imaging setpoint), recovering the alternated oxygen rows (Fig. 5B). The resulting image is then similar to those obtained at lower salt concentration or in water.

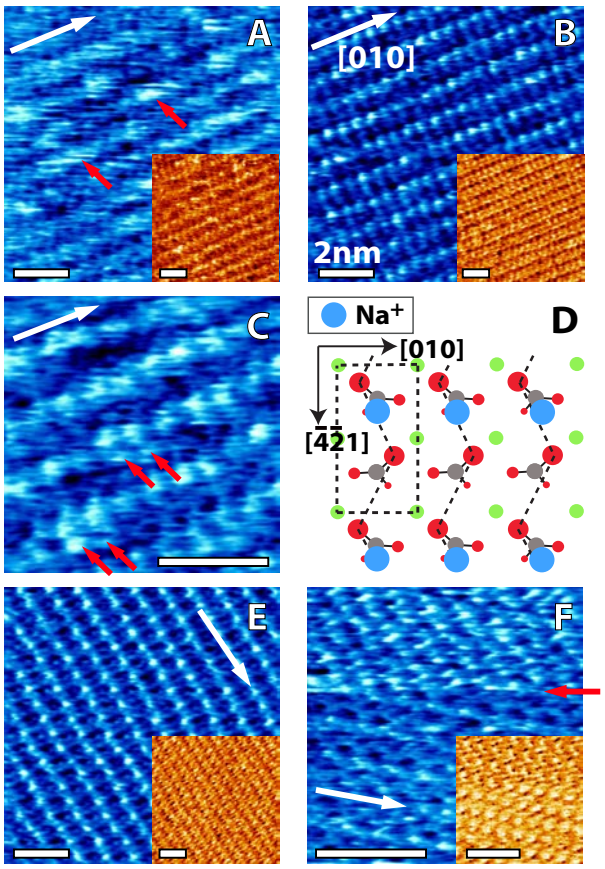

Figure 5: Calcite's $(10\bar{1}4)$ surface imaged in NaCl. The topography appears in blue and the phase is shown in inset in yellow color scale. The phase images provide an indication of the local interfacial energy with darker regions corresponding to local energy minima.[41,51] At 1 mM (E), no significant difference can be seen with AFM observations water. At 10 mM (A, C) new protrusions appear on the surface, locally broadening the prominent oxygen rows along [010] direction (red arrows). Decreasing the scanning setpoint (larger tip-sample pressure) removes the protrusions (B) and the surface once more appears similar to when imaged in water. (C) Higher resolution imaging over the protrusions suggests that they are due to adsorbed Na^+ ions, located next to the protruding oxygens, opposite the surface Ca^{2+}. (D) Cartoon representation of the presumed location of adsorbed Na^+ ions at 10 mM NaCl. Increasing the NaCl concentrations to 100 mM (F) shows a surface almost covered with ions (upper part), which can be removed using

harsher imaging conditions (red arrow, lower part). In all images, the white arrow indicates the [010] direction.

Using gentle scanning conditions we were able to obtain higher resolution images of the salt-induced protrusions (Fig. 5C, red arrow), showing the occasional adsorption of ~3 Å wide objects adjacent to the prominent oxygen atoms, opposite the underlying surface calcium ions. We attribute these objects to hydrated Na^+ ions, consistent with their location close to prominent oxygens while remaining as distant as possible from the surface calcium atoms (Fig. 5D). This observation is compatible with MD results apart for a small deviation from the MD predictions: the AFM results show the hydrated Na^+ adjacent to the prominent carbonate oxygen while the MD simulations show the Na^+ exactly on top of the oxygen (see section 3.1 and Fig.2). This small discrepancy can be explained in two different manners. Firstly, the AFM perturbs the system during the imaging process. The imaged ion is confined between the calcite surface and the AFM tip and the resulting potential minimum may not necessarily be located exactly on top of the considered oxygen atom. Na^+ ions could, nevertheless be occasionally observed forming a single protrusion with the oxygen atom (see Fig. S1 in SI). Secondly, the oxygen row pairing visible in the AFM may shift the equilibrium position with respect to the MD simulation where the row pairing is not visible.

In order to further confirm the presence of adsorbed ions at 10 mM NaCl, we acquired simultaneous amplitude and phase versus distance curves (spectroscopy) in conditions identical to those used for imaging. A selection of 10 representative curves is presented in figure 6 and compared with the same results obtained in water. In each case, one curve has been highlighted in red for discussion purposes. In water, both the amplitude and phase are very reproducible and the curves show little variation. In 10 mM NaCl, the curves show a much larger variation with

two distinct populations. The first is very similar to the curves obtained in water. The second population (red curve in Fig.6) shows a distinctive but poorly reproducible step (white arrow in Fig.6) visible in both amplitude and phase.

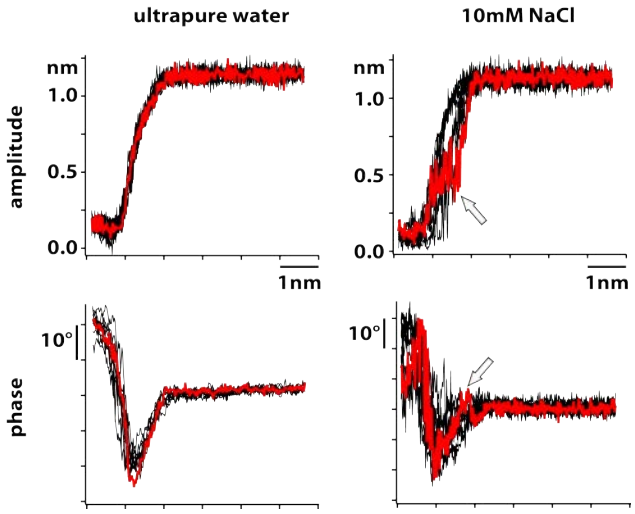

Figure 6: Amplitude and phase vs distance curves (10 curves in each case) obtained in equilibrated ultrapure water and 10 mM NaCl solution. The curves were acquired immediately after imaging. One representative curve is highlighted in red in each case.

We attribute this step to the presence of adsorbed Na^+ ions removed by the tip as it approaches the surface. The poor reproducibility of the steps comes from the weak adsorption of the ions to the surface, leading to different trajectories of the tip as it expels the ions. The ease with which the Na^+ ions can be removed suggests that they are not directly adsorbed onto the calcite surface, but separated by at least one water layer, consistent with the idea of a strongly hydrated calcite surface[3,7] also confirmed by MD simulations (see section 3.1). Hydrated Na^+ ions would have to pay an important energy penalty corresponding to the partial loss and restructuring of their hydrations shell in order to penetrate calcite's solvation structure.[7,52] We note that no clear contribution from long-range (>2-3nm) repulsive electrostatic double layer forces is visible in Fig. 6 despite working at salt concentrations below 20mM NaCl. We believe that this can be

explained by the presence of particularly sharp nanometer-size features at the tip apex. Although beneficial when probing short-range solvation forces, the net double layer force experienced by these sharp features is likely to be below our detection threshold.

At 100 mM considerably more protrusions are visible (Fig. 5F) and the "row pairing" is less clear, probably due to the adsorbed ions. Increasing the tip-sample pressure (lower setpoint) does still induce a transition (Fig. 5F, red arrow) but a direct interpretation becomes more difficult, firstly because the surface appears completely covered with ions and Cl^- ions may have to be considered to ensure charge neutrality, and secondly because the surface charge of the tip may artificially increase the apparent ionic coverage. This second effect becomes evident in $CaCl_2$ (section 3.4).

3.3 AFM of calcite in Rubidium Chloride.

In order to further substantiate our findings, we repeated the experiment with RbCl, a different monovalent salt. The choice of RbCl is motivated first by the Rb^+ large size and loose hydration shell. If verified, the dehydration argument developed for the adsorbed Na^+ ions should allow Rb^+ ions to sit even closer to the calcite's surface. Second, AFM results obtained with Rb^+ ions may provide a point of comparison for future diffraction experiments where Rb^+ ions are usually preferred.[8] The main results are presented in figure 7.

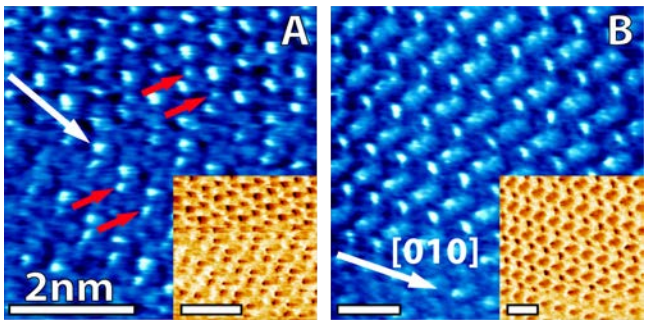

Figure 7. Calcite's $(10\bar{1}4)$ surface imaged in RbCl. The color scales and image presentations are as for Fig.5. At 10 mM (A), additional protrusions in the unit cell of the calcite crystal are visible along the [010] direction (red arrows). When increasing the RbCl concentration, the protrusions progressively merge together and a simple interpretation of the height contrast becomes difficult. At 100 mM (B), a reconstruction of the surface is visible with a lattice periodicity doubled in both the [010] and the $[\bar{4}\bar{2}1]$ directions. The white arrow indicates the [010] direction.

At low RbCl concentration (<5 mM) the surface of calcite appears similar to when observed in equilibrated pure water, with the paired oxygen rows (Fig. S2A, SI). At 10 mM RbCl, additional protrusions appear on the surface. Their location coincides with that of Na^+ ions in NaCl experiments (Fig. 7A, red arrows), but the protrusions, attributed to the Rb^+ ions, are clearer and better defined. Adsorbed Rb^+ ions are also more resistant to the scanning AFM tip, consistent with the dehydration argument where ions possessing a looser hydration shell stay closer to the calcite surface.

Similarly to in NaCl, the adsorbed cations can be removed at low salt concentration when increasing the pressure exerted by the tip on the imaged surface. Interestingly, the "row-pairing" is not clear anymore (Fig. 7A) but the adsorbed Rb^+ still appear to follow the pairing by adsorbing only every other oxygen row along the [010] direction. As the salt concentration increases, the surface of calcite progressively restructures dramatically (see Fig. S2 SI) achieving a unit cell twice as large at 100 mM (Fig. 7B and S2C-D, SI). A substantial decrease of the imaging setpoint (harsher imaging conditions) allows the recovery of an apparent "row-pairing" (Fig. 7B) but the inter-row dimension is still doubled. The Rb^+-induced single protrusions broaden and merge with that of the neighboring oxygen, forming a single solvation structure. Although full interpretation of this dramatic restructuring may require complementary insight

from diffraction techniques, these results confirm the trend observed in NaCl and support the idea that hydration effects dominate the energy required for ions and charged molecules to approach the surface of calcite.

3.4 AFM of calcite in Calcium Chloride.

High concentrations of calcium can be found in seawater as well as in certain rivers, prompting us to investigate the surface of calcite in the presence of $CaCl_2$. Furthermore, when at equilibrium in water, calcium ions dissolve from the calcite into the water, typically reaching concentrations of 0.4 mM under normal atmospheric conditions. Since Ca^{2+} is a divalent ion, its solvation shell is larger than that of monovalent cations. Ca^{2+} can therefore be expected to pay a larger energy penalty for dehydration than Na^+ and Rb^+ to reach the surface of calcite. AFM images of the calcite surface in $CaCl_2$ are presented in Fig. 8. At 1 mM $CaCl_2$, the ionic strength of the solution is higher but still comparable to that naturally present in ultrapure water after equilibration, and the surface of the calcite appear similar (Fig. 8A).

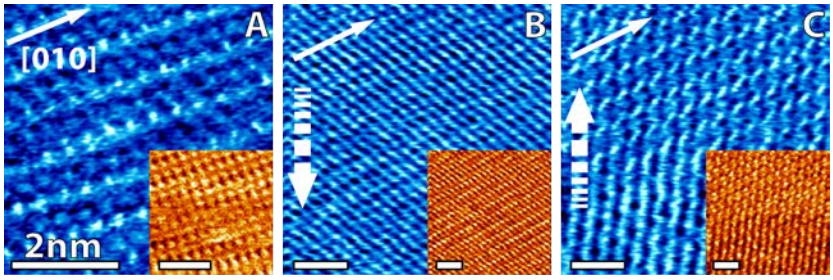

Figure 8. Calcite's $(10\bar{1}4)$ surface imaged in $CaCl_2$. The color scales and image presentations are as for Fig. 5. At 1 mM (A), the surface of calcite appears similar to the way it appears in water. At 10 mM tip-induced effects become important and two consecutive AFM images acquired from top to bottom (B) and bottom to top (C) can look different, although the underlying

symmetry is preserved. The full white arrows indicate the [010] direction and the large dotted arrows in (B) and (C) indicate the direction of the slow scan axis.

At 10 mM $CaCl_2$, the calcite surface appears different, with lines following the crystal lattice instead of distinct surface atoms that are often no longer visible (Fig. 8B-C). Although the imaged structure is correlated with calcite's lattice, it is clearly influenced by the scanning tip; two images acquired consecutively show different structures (Fig. 8B-C). In figure 8C, the familiar "row pairing" is recovered toward the end of the image acquisition (upper part). This result indicates that the divalent Ca^{2+} ions interact more weakly with the surface of calcite than the monovalent Na^+ and Rb^+ ions, consistently with a dehydration-dominated interaction (see section 3.2 and 3.3). As a result, the AFM tip can easily push the loosely adsorbed but strongly hydrated Ca^{2+} ions as it scans across the surface. The charge distribution at calcite's surface then becomes a guiding potential landscape for the ions, which tend to follow preferential directions (the lines) when confined between the tip and the crystal. The negative surface charge of the SiN tip will also affect divalent Ca^{2+} ions more than monovalent ions. This suggests that the resulting images can be seen as maps of calcite surface potential probed by tip-bound hydrated Ca^{2+} ions.

3.5 General discussion.

The MD observations correspond well overall with the experimental results, especially when taking into account the difference in hydration shell for the Na^+- and Ca^{2+}-ions, which were computed from ions remaining in the bulk water. The coordination numbers of water molecules (around 6 for Na^+ and 8 for Ca^{2+}) showed a larger hydration shell for Ca^{2+}, which is in line with the fact that in order to get closer to the calcite-water interface a higher energy barrier must be overcome. The simulation results also indicated two highly ordered water layers at a distance of

222 pm and 330 pm from calcite's surface calcium atoms. These water layers prevent the ions in solutions from approaching the surface over flat areas: the main mechanism, observed experimentally in this paper, originates from the energy penalty the ions have to pay due to the removal of their hydration shell and the breaking of the "ice-like" water layer on the surface of calcite.[52] A second mechanism may also play a role: the ordering of the water layers creates an alternation of positive and negative charge excess in the direction perpendicular to the surface, due to the oxygen and hydrogen atoms of the oriented water molecules.[52] This alternation creates a modulation of the free energy barrier experienced by ions approaching the surface. The barrier, observed in simulations studies,[52] depends mainly on the ion charge density. Monovalent cations experience a lower free energy barrier compared to divalent ions, but the nature of the considered ions has to be taken into account when considering the dehydration energy penalty. Our AFM results suggest that sodium and rubidium ions are favorable in the interaction with the calcite surface compared to calcium and can come closer to the surface. Our images also provide preferential locations for these ions, when close to the calcite surface. These findings are confirmed by MD simulation in the case of sodium and calcium. It is important, however, to realize that these hydration-dominated effects depend strongly on the interface considered. In the present case, the particular orientation and ordering of the water molecules close to the surface of calcite leads to the observed hydration-dominated ion adsorption. This is related to the specific charge distribution at the surface of calcite; surfaces with a different local charge distribution can allow electrostatic interaction to dominate ion adsorption, despite the presence of ordered water layers. This is, for example, the case for mica in water[55]. Both monovalent (Li^+ and Na^+) and divalent (Mg^{2+} and Ca^{2+}) ions have been shown to interact strongly with the surface of mica and could consequently be imaged with AFM.[56]

From the MD simulation results we were able to compute the residence time of the different ions within a certain distance from the calcite surface (vertical mobility). The distance was selected so as to match maxima in the density peak of the considered type of ion (see Fig. 3(B)). Although the derived numbers must be considered cautiously, they provide a good point of comparison for differences in mobility between the considered ionic species close to calcite's surface. Calcium ions reside approximately 750 ps at their density peak (~550 pm from the calcium atoms of the calcite surface). Chloride ions reside around 475 ps at their first density peak (~480 pm from the calcium atoms of the calcite surface) while the sodium ions remain for more than 5ns at their first density peak (~290 pm from the calcium atoms of the calcite surface), exceeding the duration of the entire simulation run. Estimations of the ions lateral mobility (parallel to the calcite surface) when "trapped" in the first water layers of the calcite surface were difficult to derive, but we estimated that the diffusion coefficient for sodium ions was decreased by at least a factor 200 with respect to the bulk value. In the case of calcium ions, the lateral diffusivity was typically one order of magnitude lower than in the bulk but still one order of magnitude bigger than the lateral diffusivity of sodium ions at their first density peak. These observations are consistent with the differences observed in the AFM imaging of the different ions where the possibility to distinguish single ions seems to be a prerogative of the monovalent Na^+ and Rb^+ ions. Caution should however be exerted when comparing AFM and the MD results since the MD simulations presented here do not take into account the fact that the interfacial liquid is effectively confined between the calcite surface and the AFM tip under typical imaging conditions. Recent MD simulation studies have shown that under confinement, the liquid can exhibit substantial changes in its viscoelastic properties and molecular dynamics,[57] and induce ion-specific structures.[58] The good correspondence between the trends derived from

AFM and the present MD simulations results suggests that AFM can nevertheless capture the main features of the 'non-confined' interface. This could be explained by the AFM having a particularly sharp tip apex, hence limiting confinement and enhancing resolution.

Our results also bring new insights into the important problem of Electrical Double Layer (EDL) at the surface of calcite. This model defines the Stern layer as the plane where the outer-sphere complexation of 'adsorbed' ions is located. The determination of the thickness of the Stern layer, and particularly of the plane where the outer-sphere complexation is assumed to take place is essential for the modeling of the EDL.[3,7,37] Our results show that, depending on the ions considered, the position at which the complexation with the calcite surface takes place varies substantially. The Na^+ ions are able to come closer to the surface while Ca^{2+} and Cl^- ions stay further apart. Moreover, the actual vertical mobility of the ionic species, as discussed in the previous paragraph, is very different and we propose this mobility as an important parameter to consider when the outer-sphere complexation of 'adsorbed' ions has to be determined in the model.

Finally, our results suggest that the ion-specific effects observed on calcite can be used as a model system to study ion-specific hydration effects in a more general context. Similar effects are observed for very different systems such as ion-specific hydration effects at hydrophobic surfaces.[59] The analysis of interfacial phenomena at the nano-scale often requires to consider the specifics of hydration and continuum classical theory may no longer be valid.[60]

4. CONCLUSION

In this paper we explored the interface between calcite ($10\bar{1}4$) and different ionic solutions combining AFM experiments and MD simulations. We provide the first high-resolution AFM

images of hydrated Na^+ and Rb^+ ions adsorbed close to the $(10\bar{1}4)$ surface of calcite in aqueous solution, away from atomic steps. The cations preferential adsorption site appears to be located close to the prominent oxygen atoms of the surface carbonate groups, opposite the underlying calcium. The surface of calcite is strongly hydrated and the approaching ions have to pay a substantial energy penalty incurred by the loss or restructuring of their hydration shell when traversing calcite's ice-like hydration layers. MD simulation shows that this energy penalty prevents hydrated ions from directly adsorbing onto the surface, which always retains at least one undisturbed water layer. Divalent ions such as Ca^{2+} stay even further from the surface due to their large hydration shell, thus preventing AFM imaging from identifying a preferential location for the Ca^{2+} ion close to the surface. Future high-resolution studies will concentrate on edge effects where Calcite's solvation structure is known to break down and where different ions can interact directly with the surface.[34,61]

ASSOCIATED CONTENT

Supporting Information.

Supporting Information. Additional experimental details and AFM images of the surface of calcite in the presence of Na^+ and Rb^+ ions. A detailed description of the evolution of the surface with increasing concentrations of RbCl is also provided.

This material is available free of charge via the Internet at http://pubs.acs.org."

AUTHOR INFORMATION

Corresponding Author

e-mail address: kislon.voitchovsky@epfl.ch

Author Contributions

The manuscript was written with contributions from all authors. All authors have given approval to the final version of the manuscript.

Funding Sources

This work has been supported by funding from the Swiss National Science Foundation through the Ambizione Award no PZ00P2_136941 (KV). PS and JFM acknowledge the support of European Research Council Starting Grant no 240332

ACKNOWLEDGMENT

We acknowledge Dr. Frank Heberling for useful discussions regarding the experiments and the results. The experimental work was conducted as part of an ongoing collaboration with Shell petroleum.

REFERENCES

(1) Heberling, F.; Trainor, T. P.; Lützenkirchen, J.; Eng, P.; Denecke, M. A.; Bosbach, D. *J. Structure and reactivity of the calcite–water interface. Coll. Interf Sci.* **2011**, *354*, 843-857.

(2) Kuffner, I. B.; Andersson, A. J. Jokiel, P. L.; Rodgers, K. U. S.; Mackenzie, F. T. Decreased abundance of crustose coralline algae due to ocean acidification. *Nat. Geosci.* **2007**, *1*, 114-117.

(3) Andersson, A. J.; Mackenzie, F. T.; Bates, N. R. Life on the margin: implications of ocean acidification on Mg-calcite, high latitude and cold-water marine calcifiers. *Mar. Ecol. Prog. Ser.* **2008**, *373*, 265-273.

(4) Archer, D.; Maier-Reimer, E. Effect of deep-sea sedimentary calcite preservation on atmospheric CO_2 concentration. *Nature* **1994**, *367*, 260-263.

(5) Choi, W. H.; Shin, J. W.; Kim, J. J.; Park, J. Y. Calcite-packed columns for the removal of fluoride in industrial wastewater. *Desalin. Water Treat.* **2011**, *30*, 247-253.

(6) Zullig, J. J.; Morse, J. W. Interaction of organic acids with carbonate mineral surfaces in seawater and related solutions: I. Fatty acid adsorption. *Geochim. Cosmochim. Acta* **1988**, *52*, 1667-1678.

(7) Stipp, S. L. S. Toward a conceptual model of the calcite surface: hydration, hydrolysis, and surface potential. *Geochim. Cosmochim. Acta* **1999**, *63*, 3121-3131.

(8) Geissbühler, P.; Fenter, P.; DiMasi, E.; Srajer, G.; Sorensen, L. B.; Sturchio, N. C. Three-dimensional structure of the calcite–water interface by surface X-ray scattering. *Surf. Sci.* **2004**, *573*, 191-203.

(9) Ruiz-Agudo, E.; Putnis, C. V. Direct observations of mineral–fluid reactions using atomic force microscopy: the specific example of calcite. *Mineral. Mag.* **2012**, *76*, 227-253.

(10) Kerisit, S.; Parker, S. C. Free Energy of Adsorption of Water and Metal Ions on the $\{10\bar{1}4\}$ Calcite Surface. *J. Am. Chem. Soc.* **2004**, *126*, 10152-10161.

(11) Yang, M.; Mark Rodger, P.; Harding, J. H.; Stipp, S. L. S. Molecular dynamics simulations of peptides on calcite surface. *Molec. Simulation* **2009**, *35*, 547-553.

(12) Thomas, M. M.; Clouse, J. A.; Longo, J. M. Adsorption of organic compounds on carbonate minerals: 1. Model compounds and their influence on mineral wettability. *Chem. Geology* **1993**, *109*, 201-213.

(13) Stipp, S. L. S.; Konnerup-Madsen, J.; Franzreb, K.; Kulik, A.; Mathieu, H. J. Spontaneous movement of ions through calcite at standard temperature and pressure. *Nature* **1998**, *396*, 356-359.

(14) Harstad, A. O.; Stipp, S. L. S. Calcite dissolution: Effects of trace cations naturally present in Iceland spar calcites. *Geochim. Cosmochim. Acta* **2007**, *71*, 56-70.

(15) Vavouraki, A. I.; Putnis, C. V.; Putnis, A.; Koutsoukos, P. G. Crystal Growth and Dissolution of Calcite in the Presence of Fluoride Ions: An Atomic Force Microscopy Study. *Cryst. Growth & Design* **2010**, *10*, 60-69.

(16) Karoussi, O.; Skovbjerg, L. L.; Hassenkam, T.; Stipp, S. L. S.; Hamouda, A. A. AFM study of calcite surface exposed to stearic and heptanoic acids. *Coll. Surf. A* **2008**, *325*, 107-114.

(17) Maslen, E. N.; Streltsov, V. A.; Streltsova, N. R. X-ray study of the electron density in calcite, $CaCo_3$. *Acta Crystallogr. B Struct Sci* **1993**, *49*, 636-641.

(18) Schütte, J.; Rahe, P.; Tröger, L.; Rode, S.; Bechstein, R.; Reichling, M.; Kühnle, A. Clear Signature of the (2×1) Reconstruction of Calcite $(10\bar{1}4)$. *Langmuir* **2010**, *26*, 8295-8300.

(19) Rahe, P.; Schütte, J.; Kühnle, A. NC-AFM contrast formation on the calcite $(10\bar{1}4)$ surface. *J. Phys.: Condens. Matter* **2012**, *24*, 084006(14pp).

(20) Stipp, S. L. S.; Eggleston, C. M.; Nielsen, B. S. Calcite surface structure observed at microtopographic and molecular scales with atomic force microscopy (AFM). *Geochim. Cosmochim. Acta* **1994**, *58*, 3023-3033.

(21) Ohnesorge, F. Towards atomic resolution non-contact dynamic force microscopy in a liquid. *Surf. Interface Anal.* **1999**, *27*, 379-385.

(22) Rode, S.; Oyabu, N.; Kobayashi, K.; Yamada, H.; Kühnle, A. True Atomic-Resolution Imaging of $(10\bar{1}4)$ Calcite in Aqueous Solution by Frequency Modulation Atomic Force Microscopy. *Langmuir* **2009**, *25*, 2850-2853.

(23) Stipp, S.; Hochella, M. Structure and bonding environments at the calcite surface as observed with X-ray photoelectron spectroscopy (XPS) and low energy electron diffraction (LEED). *Geochim. Cosmochim. Acta* **1991**, *55*, 1723-1736.

(24) Fenter, P.; Geissbühler, P.; DiMasi, E.; Srajer, G. Surface speciation of calcite observed in situ by high-resolution X-ray reflectivity. *Geochim. Cosmochim Acta* **2000,** 64, 1221-1228.

(25) Gratz, A. J.; Hillner, P. E. Poisoning of calcite growth viewed in the atomic force microscope (AFM). *J. Cryst. Growth* **1993***, 129*, 789-793.

(26) Davis, K. J.; Dove, P. M.; De Yoreo, J. J. The role of Mg^{2+} as an impurity in calcite growth. *Science* **2000**, *290*, 1134-1137.

(27) Bisschop, J.; Dysthe, D. K.; Putnis, C. V.; Jamtveit, B. In situ AFM study of the dissolution and recrystallization behavior of polished and stressed calcite surfaces. *Geochim. Cosmochim. Acta* **2006**, *70*, 1728-1738.

(28) De Yoreo, J. J.; Zepeda-Ruiz, L. A.; Friddle, R. W.; Qiu, S. R.; Wasylenki, L. E.; Chernov, A. A.; Gilmer, G. H.; Dove, P. M. Rethinking Classical Crystal Growth Models through Molecular Scale Insights: Consequences of Kink-Limited Kinetics. *Cryst. Growth & Design* **2009**, *9*, 5135-5144.

(29) Bohr, J.; Wogelius, R. A.; Morris, P. M.; Stipp, S. L. S. Thickness and structure of the water film deposited from vapour on calcite surfaces. *Geochim. Cosmochim. Acta* **2010**, *74*, 5985-5999.

(30) Kristensen, R.; Stipp, S. L. S.; Refson, K. Modeling steps and kinks on the surface of calcite. *J. Chem. Phys.* **2004**, *121*, 8511-8523.

(31) Ruiz-Agudo, E.; Putnis, C. V.; Rodriguez-Navarro, C.; Putnis, A. Effect of pH on calcite growth at constant ratio and supersaturation. *Geochim. Cosmochim. Acta* **2010**, *75*, 284-296.

(32) Ruiz-Agudo, E.; Putnis, C. V.; Wang, L.; Putnis, A. Specific effects of background electrolytes on the kinetics of step propagation during calcite growth. *Geochim. Cosmochim. Acta* **2011**, *75*, 3803-3814.

(33) Wang, L.; Ruiz-Agudo, E.; Putnis, C. V.; Putnis, A. Direct observations of the modification of calcite growth morphology by Li+ through selectively stabilizing an energetically unfavourable face. *CrystEngComm* **2011**, *13*, 3962-3966.

(34) de Leeuw, N. H. Molecular Dynamics Simulations of the Growth Inhibiting Effect of Fe^{2+}, Mg^{2+}, Cd^{2+}, and Sr^{2+} on Calcite Crystal Growth. *J. Phys. Chem. B* **2002**, *106*, 5241-5249.

(35) Wasylenki, L. E.; Dove, P. M.; Wilson, D. S.; De Yoreo, J. J. Nanoscale effects of strontium on calcite growth: An in situ AFM study in the absence of vital effects. *Geochim. Cosmochim. Acta* **2005**, *69*, 3017-3027.

(36) Arvidson, R. S.; Collier, M.; Davis, K. J.; Vinson, M. D.; Amonette, J. E.; Luttge, A. Magnesium inhibition of calcite dissolution kinetics. *Geochim. Cosmochim. Acta* **2005**, *70*, 583-594.

(37) Chen, C.-L.; Qi, J.; Zuckermann, R. N.; DeYoreo, J. J. Engineered Biomimetic Polymers as Tunable Agents for Controlling $CaCO_3$ Mineralization. *J. Am. Chem. Soc.* **2011**, *133*, 5214-5217.

(38) Elhadj, S.; De Yoreo, J. J.; Hoyer, J. R.; Dove, P. M. Role of molecular charge and hydrophilicity in regulating the kinetics of crystal growth. *Proc. Natl. Acad. Sci. U.S.A* **2006**, *103*, 19237-19242.

(39) Rahe, P.; Schütte, J.; Kühnle, A. NC-AFM contrast formation on the calcite ($10\bar{1}4$) surface. *J. Phys.: Condens. Matter* **2012**, *24*, 084006(14pp).

(40) Freeman, C. L.; Harding, J. H.; Cooke, D. J.; Elliott, J. A.; Lardge, J. S.; Duffy, D. M. New Forcefields for Modeling Biomineralization Processes. *J. Phys. Chem. C* **2007**, *111*, 11943-11951.

(41) Voïtchovsky, K.; Kuna, J. J.; Contera, S. A.; Tosatti, E.; Stellacci, F. Direct mapping of the solid-liquid adhesion energy with subnanometre resolution. *Nature Nanotechnol.* **2010**, *5*, 401-405.

(42) Stöckelmann, E.; Hentschke, R. Adsorption Isotherms of Water Vapor on Calcite: A Molecular Dynamics–Monte Carlo Hybrid Simulation Using a Polarizable Water Model. *Langmuir* **1999**, *15*, 5141-5149.

(43) Dove, M. T.; Winkler, B.; Leslie, M.; Harris, M. J.; Salje, E. K. H. A new interatomic potential model for calcite: applications to lattice dynamics studies, phase transition, and isotope fractionation. *American Mineralogist* **1992**, *77*, 244-250.

(44) MacKerell A D; Bashford, D.; Bellott; Dunbrack R L; Evanseck, J. D.; Field, M. J.; Fischer, S.; Gao, J.; Guo, H.; Ha, S.; Joseph-McCarthy, D.; Kuchnir, L.; Kuczera, K.; Lau, F. T. K.; Mattos, C.; Michnick, S.; Ngo, T.; Nguyen, D. T.; Prodhom, B.; Reiher, W. E.; Roux, B.; Schlenkrich, M.; Smith, J. C.; Stote, R.; Straub, J.; Watanabe, M.; Wiórkiewicz-Kuczera, J.; Yin, D.; Karplus, M. All-Atom Empirical Potential for Molecular Modeling and Dynamics Studies of Proteins. *J. Phys. Chem. B* **1998**, *102*, 3586-3616.

(45) Mackerell, A. D. Empirical force fields for biological macromolecules: Overview and issues. *J. Comput. Chem.* **2004**, *25*, 1584-1604.

(46) Brooks, B. R.; Brooks, C. L., III; Mackerell, A. D., Jr.; Nilsson, L.; Petrella, R. J.; Roux, B.; Won, Y.; Archontis, G.; Bartels, C.; Boresch, S.; Caflisch, A.; Caves, L.; Cui, Q.; Dinner, A. R.; Feig, M.; Fischer, S.; Gao, J.; Hodoscek, M.; Im, W.; Kuczera, K.; Lazaridis, T.; Ma, J.; Ovchinnikov, V.; Paci, E.; Pastor, R. W.; Post, C. B.; Pu, J. Z.; Schaefer, M.; Tidor, B.; Venable, R. M.; Woodcock, H. L.; Wu, X.; Yang, W.; York, D. M.; Karplus, M. CHARMM: The biomolecular simulation program. *J. Comput. Chem.* **2009**, *30*, 1545-1614.

(47) Phillips, J. C.; Braun, R.; Wang, W.; Gumbart, J.; Tajkhorshid, E.; Villa, E.; Chipot, C.; Skeel, R. D.; Kalé, L.; Schulten, K. Scalable molecular dynamics with NAMD. *J. Comput. Chem.* **2005**, *26*, 1781-1802.

(48) Humphrey, W.; Dalke, A.; Schulten, K. VMD: visual molecular dynamics. *J Mol Graph* **1996**, *14*, p. 33-8, 27-8.

(49) Michaud-Agrawal, N.; Denning, E. J.; Woolf, T. B.; Beckstein, O. MDAnalysis: A toolkit for the analysis of molecular dynamics simulations. *J. Comput. Chem.* **2011**, *32*, 2319-2327.

(50) Kuna, J. J.; Voïtchovsky, K.; Singh, C.; Jiang, H.; Mwenifumbo, S.; Ghorai, P. K.; Stevens, M. M.; Glotzer, S. C.; Stellacci, F. The effect of nanometre-scale structure on interfacial energy. *Nature Materials* **2009**, *8*, 837-842.

(51) Voïtchovsky, K.; Ricci, M. Parak, W. J.; Yamamoto, K.; Osinski, M. High-resolution imaging of solvation structures with amplitude-modulation atomic force microscopy. Eds. SPIE: San Francisco, California, USA, **2012**, 8232, 82320O-1-82320O-8.

(52) Kerisit, S.; Parker, S. C. Free Energy of Adsorption of Water and Metal Ions on the $\{10\bar{1}4\}$ Calcite Surface. *J. Am. Chem. Soc.* **2004**, 126, 10152-10161.

(53) Spagnoli, D.; Cooke, D. J.; Kerisit, S.; Parker, S. C. Molecular dynamics simulations of the interaction between the surfaces of polar solids and aqueous solutions. *J Mater Chem* **2006,** 16, 1997-2006.

(54) Perry, T. D., IV; Cygan, R. T.; Mitchell, R. Molecular models of a hydrated calcite mineral surface. *Geochim. Cosmochim. Acta* **2007**, 71, 5876-5887.

(55) Fukuma, T.; Ueda, Y.; Yoshioka, S.; Asakawa, H. Atomic-Scale Distribution of Water Molecules at the Mica-Water Interface Visualized by Three-Dimensional Scanning Force Microscopy. *Phys. Rev. Lett.* **2010**, *104*, 016101

(56) Loh, S. H.; Jarvis, S. P. Visualization of Ion Distribution at the Mica–Electrolyte Interface. *Langmuir* **2010**, *26*, 9176-9178.

(57) de Beer, S.; den Otter, W. K.; van den Ende, D.; Briels, W. J., Mugele, F. Can Confinement-Induced Variations in the Viscous Dissipation be Measured? *Tribo. Lett.* **2012**, *48*, 1.

(58) Kalcher, I; Schulz, J. C. F.; Dzubiella, J. Electrolytes in a nanometer slab-confinement: Ion-specific structure and solvation forces. *J. Chem. Phys.* **2010**, *133*, 164511.

(59) Huang, D. M.; Cottin-Bizonne, C.; Ybert, C.; Bocquet, L. Aqueous Electrolytes near Hydrophobic Surfaces: Dynamic Effects of Ion Specificity and Hydrodynamic Slip. *Langmuir* **2007**, *24*, 1442-1450.

(60) Ben-Yaakov, D.; Andelman, D.; Podgornik, R.; Harries, D. Ion-specific hydration effects: Extending the Poisson-Boltzmann theory. *Curr. Op. Col. Interf. Sci.* **2011**, *16*, 542-550.

(61) Spagnoli, D.; Kerisit, S.; Parker, S. C. Atomistic simulation of the free energies of dissolution of ions from flat and stepped calcite surfaces. *J. Cryst. Growth* **2006**, *294*, 103-110.